

# Phase diagram and quench dynamics of the cluster- $XY$ spin chain

Sebastián Montes\*

*Perimeter Institute for Theoretical Physics, 31 Caroline Street North, Waterloo, Ontario, Canada N2L 2Y5 and  
University of Waterloo, 200 University Avenue West, Waterloo, Ontario, Canada N2L 3G1*

Alioscia Hamma†

*Perimeter Institute for Theoretical Physics, 31 Caroline Street North, Waterloo, Ontario, Canada N2L 2Y5*  
(Received 25 December 2011; revised manuscript received 15 June 2012; published 1 August 2012)

We study the complete phase space and the quench dynamics of an exactly solvable spin chain, the cluster- $XY$  model. In this chain, the cluster term and the  $XY$  couplings compete to give a rich phase diagram. The phase diagram is studied by means of the quantum geometric tensor. We study the time evolution of the system after a critical quantum quench using the Loschmidt echo. The structure of the revivals after critical quantum quenches presents a nontrivial behavior depending on the phase of the initial state and the critical point.

DOI: [10.1103/PhysRevE.86.021101](https://doi.org/10.1103/PhysRevE.86.021101)

PACS number(s): 75.10.Pq, 05.30.Fk, 05.30.Rt, 75.10.Dg

## I. INTRODUCTION

In recent years, the understanding of quantum phases and quantum phase transitions has gained incredible momentum. This is due to both strong theoretical advances, stimulated by the richness of quantum phases, and experimental advances. On the theoretical side, there has been great progress in understanding how quantum critical points affect the finite-temperature regime [1] and quantum entanglement [2]. Moreover, we are realizing that quantum phases host rich novel quantum orders and phases of matter [3]. From the experimental side, ultracold-atom gases have proven to be the ideal arena to see coherent quantum evolution for many-body systems [4–6].

The study of closed quantum systems out of equilibrium is important for manifold reasons. To start with, one is interested in applications to quantum information in which decoherence and entanglement dynamics play a fundamental role. An important theoretical perspective concerns the understanding of the notion of universality for a system away from equilibrium, where the traditional concepts of phase, renormalization group, and fixed point fail. Recently, the study of the equilibration of quantum many-body systems has given insight into the foundations of statistical mechanics [7–10].

Driving a system out of equilibrium can be accomplished in many ways. Most of the efforts have focused on quantum quenches [10], namely, sudden global or local changes of the external parameters of the Hamiltonian governing the unitary evolution of the closed system. One of the ways of understanding the dynamics of a system after a quench is the Loschmidt echo, which is a measure of the partial recurrences with the original state as a function of time [11,12]. Recently, the time behavior of the Loschmidt echo has been investigated in various models, in particular the  $XY$  spin chain [13–16].

In this paper we will consider a one-dimensional model that extends the  $XY$  spin chain with a three-body cluster term. The exact solution becomes available using well-known techniques and this allows us to study the complete phase diagram. We find

that a particular critical region has a behavior quite different from the one found in the  $XY$  model. We then study the behavior of the Loschmidt echo after critical quenches for two different critical points. We find qualitative differences derived from the nontrivial nature of the phase space.

## II. CLUSTER- $XY$ SPIN CHAIN

Cluster states have emerged recently as a physical system for implementing one-way quantum computation. In particular, it has been shown that two-dimensional cluster states serve as fiducial states for universal measurement-based quantum computation [17–21].

The cluster state can be defined using a so-called stabilizer Hamiltonian. Consider a finite-dimensional lattice  $\mathbb{L}$  composed of  $N$  vertices, each vertex containing a two-dimensional quantum system (qubit). The cluster state for this system can be defined as the unique  $+1$  eigenstate of the stabilizer operators

$$K_\mu = \sigma_\mu^z \prod_{\nu \sim \mu} \sigma_\nu^x, \quad \mu, \nu \in \mathbb{L}, \quad (1)$$

where  $\nu \sim \mu$  denotes that  $\nu$  is connected to  $\mu$  and  $\sigma^\alpha$  are the Pauli matrices [22]. The stabilizer Hamiltonian is simply

$$H_C = - \sum_{\mu \in \mathbb{L}} K_\mu$$

and the cluster state is defined as its ground state. This preparation can also be achieved by preparing all the qubits in the  $|0\rangle$  state ( $\sigma^z |0\rangle = |0\rangle$ ) and then performing a controlled sign operator  $U = \exp(i\pi |+\rangle \langle +| \otimes |+\rangle \langle +|)$  (where  $\sigma^x |+\rangle = |+\rangle$ ) on every pair of connected vertices [23]. The model we study incorporates the one-dimensional version of the cluster phase competing with the  $XY$  model in a transverse field. The Hamiltonian is

$$H = - \sum_{i=1}^N \sigma_{i-1}^x \sigma_i^z \sigma_{i+1}^x - h \sum_{i=1}^N \sigma_i^z + \lambda_y \sum_{i=1}^N \sigma_i^y \sigma_{i+1}^y + \lambda_x \sum_{i=1}^N \sigma_i^x \sigma_{i+1}^x, \quad (2)$$

\* smontesvalencia@perimeterinstitute.ca

† ahamma@perimeterinstitute.ca

where  $\sigma_n^\alpha$  ( $\alpha = x, y, z$ ) are the Pauli matrices acting on the site  $n$  of the lattice and we impose periodic boundary conditions ( $\sigma_{N+1}^\alpha \equiv \sigma_1^\alpha$ ). Similar models were considered in Refs. [22–25]. Defining local raising and lowering operators  $\sigma_n^\pm = \frac{1}{2}(\sigma_n^x \pm i\sigma_n^y)$ , we obtain global canonical anticommutation relations by using a Jordan-Wigner transformation [1]

$$c_l^\dagger = \left( \prod_{m=1}^{l-1} \sigma_m^z \right) \sigma_l^+, \quad (3)$$

so that the model is mapped to a quadratic Hamiltonian of spinless fermions  $\{c_n, c_m\} = 0, \{c_n, c_m^\dagger\} = \delta_{nm}$ . Note that the parity operator  $Q \equiv \prod_n \sigma_n^z$  commutes with the Hamiltonian and can be diagonalized simultaneously with it. Using the fact that the system has translational invariance, we may perform a Fourier transform

$$c_k = \frac{1}{\sqrt{N}} \sum_{n=1}^N e^{ikn} c_n, \quad k = \frac{\pi}{N}(2m+1-q),$$

where we decompose the Hilbert space so that  $Q = (-1)^q$  and  $m = 0, \dots, N-1$ . We can then rewrite the Hamiltonian as

$$H = 2 \sum_{0 \leq k \leq \pi} [\epsilon_k (c_k^\dagger c_k + c_{-k}^\dagger c_{-k}) + i\delta_k (c_k^\dagger c_{-k}^\dagger + c_k c_{-k})]$$

up to a constant, where

$$\epsilon_k = \cos(2k) - (\lambda_x + \lambda_y) \cos(k) - h, \quad (4a)$$

$$\delta_k = \sin(2k) - (\lambda_x - \lambda_y) \sin(k). \quad (4b)$$

We diagonalize the Hamiltonian by means of a Bogoliubov transformation

$$\gamma_k = \cos(\theta_k/2) c_k - i \sin(\theta_k/2) c_{-k}^\dagger, \quad (5)$$

imposing  $\theta_{-k} = -\theta_k$  so that  $\{\gamma_k, \gamma_{k'}^\dagger\} = \delta_{kk'}$ . The Hamiltonian becomes

$$H = 2 \sum_{0 \leq k \leq \pi} \Delta_k (\gamma_k^\dagger \gamma_k + \gamma_{-k}^\dagger \gamma_{-k} - 1) + \text{const}, \quad (6)$$

where we define the energy for the so-called Bogoliubov quasiparticles  $\Delta_k = \sqrt{\epsilon_k^2 + \delta_k^2}$  and cancel the unwanted  $\gamma\gamma$  terms by choosing  $\epsilon_k \sin \theta_k + \delta_k \cos \theta_k = 0$  or, equivalently,

$$\theta_k = -\arctan\left(\frac{\delta_k}{\epsilon_k}\right). \quad (7)$$

The ground state has the form of a BCS state in terms of the original operators

$$|\Omega\rangle = \prod_{0 \leq k \leq \pi} [\cos(\theta_k/2) + i \sin(\theta_k/2) c_k^\dagger c_{-k}^\dagger] |0\rangle_c, \quad (8)$$

where  $c_k |0\rangle_c = 0 \forall k$ .

### III. PHASE DIAGRAM

At this point, we can draw the phase diagram by finding the regions of quantum criticality where the system becomes gapless in the thermodynamics limit, that is,  $\Delta_k = 0$  for some  $k \in [-\pi, \pi)$  when  $N \rightarrow \infty$ . First, note that trivially  $\delta_k = 0$  for  $k = 0, \pm\pi$ . In that case,  $\epsilon_k$  vanishes for

$$h = \pm(\lambda_x + \lambda_y) + 1. \quad (9)$$

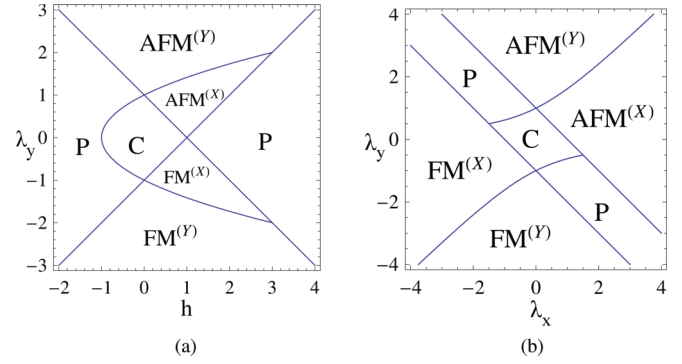


FIG. 1. (Color online) Reduced phase diagrams for (a)  $\lambda_x = 0$  and (b)  $h = 0$ . We use the following conventions: P, polarized, given by  $\sum \sigma^z$ ; C, cluster; AFM, antiferromagnetic; and FM, ferromagnetic.

Now, if  $k \neq 0, \pi$ ,  $\delta_k$  vanishes if  $\cos(k) = \frac{\lambda_x - \lambda_y}{2}$ . Using this relation for  $\epsilon_k$ , we get the critical region

$$h = \lambda_y^2 - \lambda_x \lambda_y - 1, \quad -2 \leq \lambda_x - \lambda_y \leq 2. \quad (10)$$

We see an asymmetry between  $\lambda_x$  and  $\lambda_y$ . This should be no surprise as this is already evident in the cluster term of the Hamiltonian. Note also that the union of the critical regions is invariant under  $\lambda_y \mapsto -\lambda_y, \lambda_x \mapsto -\lambda_x$ . We can understand this by noting that both local unitary transformations

$$U_1 : \sigma_{2n}^x \mapsto -\sigma_{2n}^x, \quad \sigma_{2n}^y \mapsto -\sigma_{2n}^y, \quad \sigma_{2n}^z \mapsto \sigma_{2n}^z$$

acting only on even sites and

$$U_2 : \sigma_{2n+1}^x \mapsto -\sigma_{2n+1}^x, \quad \sigma_{2n+1}^y \mapsto -\sigma_{2n+1}^y, \quad \sigma_{2n+1}^z \mapsto \sigma_{2n+1}^z$$

acting only on odd sites map  $H(\lambda_x, \lambda_y, h)$  to  $H(-\lambda_x, -\lambda_y, h)$ . This is a consequence of the  $\mathbb{Z}_2 \times \mathbb{Z}_2$  symmetry of the cluster state implemented precisely by  $U_1$  and  $U_2$  [25].

One of the interesting features of this model is the existence of phases that appear because of the competition between the XY and cluster terms. Consider first  $\lambda_x = 0$  [Fig. 1(a)]. The Hamiltonian in this case does not have Ising interactions of the type  $\sigma_n^x \sigma_{n+1}^x$ . However, two of the regions next to the cluster phase can be connected adiabatically to ferromagnetic and antiferromagnetic states in the  $x$  direction, respectively. Something similar happens for  $h = 0$ . The Hamiltonian does not have a transverse term that tries to polarize all the spins in the same  $z$  direction, nevertheless this phase is present in the reduced phase diagram [Fig. 1(b)].

### IV. FIDELITY SUSCEPTIBILITY

The phase diagram can be studied [26] by considering the fidelity susceptibility introduced in Ref. [27], namely, the response of the ground state to small changes of the external parameters. Consider a many-body system described by a Hamiltonian

$$H(\lambda) = H_0 + \lambda H_I, \quad (11)$$

where  $\lambda$  is an external parameter used to control the system. There is no loss of generality if we write the Hamiltonian this way, especially if the system is large enough so that the critical point is well localized. Here  $H_I$  is called the driving Hamiltonian. We may now diagonalize the system and obtain

both the energy spectrum and the eigenstates

$$H(\lambda) |n(\lambda)\rangle = E_n(\lambda) |n(\lambda)\rangle. \quad (12)$$

If we change  $\lambda$  to  $\lambda + \delta\lambda$  and we are away from possible critical points, the physics described by the neighboring ground states will be similar. However, note that in the thermodynamic limit different ground states will become orthogonal, as was realized by Anderson in the so-called orthogonality catastrophe [28]. For finite-size systems, we expect that the new ground state will remain close to the original ground state and we may study how fast the overlap goes to zero. In order to quantify this notion we use the fidelity [27,29]

$$\mathcal{F}(\lambda, \lambda') \equiv |\langle \Omega(\lambda) | \Omega(\lambda') \rangle|, \quad (13)$$

where  $|\Omega(\lambda)\rangle$  represents the ground state of  $H(\lambda)$ . The response of the fidelity after an infinitesimal change of the external parameter up to second order reads

$$\mathcal{F}(\lambda, \lambda + \delta\lambda) = 1 - \frac{\delta\lambda^2}{2} \chi_F + O(\delta\lambda^4), \quad (14)$$

where the fidelity susceptibility [29–31] is defined by

$$\chi_F(\lambda) \equiv \langle \partial_\lambda \Omega(\lambda) | \partial_\lambda \Omega(\lambda) \rangle - \langle \partial_\lambda \Omega(\lambda) | \Omega(\lambda) \rangle \langle \Omega(\lambda) | \partial_\lambda \Omega(\lambda) \rangle. \quad (15)$$

If we have more than one external parameter, we may generalize this result and obtain the so-called quantum geometric tensor [31]

$$T_{ab} \equiv \langle \partial_{\lambda_a} \Omega(\lambda) | \partial_{\lambda_b} \Omega(\lambda) \rangle - \langle \partial_{\lambda_a} \Omega(\lambda) | \Omega(\lambda) \rangle \langle \Omega(\lambda) | \partial_{\lambda_b} \Omega(\lambda) \rangle. \quad (16)$$

In general, this tensor will be complex. Both the real and imaginary parts have nice physical interpretations [26]. The real part will be an induced Riemannian metric on the manifold of parameters

$$g_{ab} \equiv \text{Re}(T_{ab}). \quad (17)$$

The geodesics with respect to this metric give information about the optimal adiabatic path that connects to points inside the same quantum phase. Also, the scalar curvature may be used to distinguish different phases and characterize the behavior of critical regions [26]. The imaginary part is related to the appearance of geometrical phases through the Berry curvature

$$\begin{aligned} F_{ab} &\equiv \text{Im}(T_{ab}) \\ &= \langle \partial_{\lambda_a} \Omega(\lambda) | \partial_{\lambda_b} \Omega(\lambda) \rangle - \langle \partial_{\lambda_b} \Omega(\lambda) | \partial_{\lambda_a} \Omega(\lambda) \rangle \\ &= \partial_a A_b - \partial_b A_a, \end{aligned} \quad (18)$$

where  $A \equiv \langle \Omega | \partial_{\lambda_b} \Omega \rangle$  is the adiabatic Berry connection [31,32].

Returning to the cluster-Ising model, we may compute the fidelity between neighboring ground states  $|\Omega(\lambda_i)\rangle$  (8) for different values of  $\{\lambda_i\}$ . If we change the external parameters  $\lambda_i^{(1)} \rightarrow \lambda_i^{(2)}$ , we can express the “old” ground state  $|\Omega(\lambda_i^{(1)})\rangle$  in terms of the operators that diagonalize the “new” Hamiltonian  $H(\lambda_i^{(2)})$ . The form of the wave function remains the same,

$$|\Omega(\lambda_i^{(1)})\rangle = \prod_{k>0} \left[ \cos\left(\frac{\chi_k}{2}\right) + i \sin\left(\frac{\chi_k}{2}\right) \gamma_k^\dagger \gamma_{-k}^\dagger \right] |\Omega(\lambda_i^{(2)})\rangle, \quad (19)$$

where  $\gamma_k$  and  $\gamma_k^\dagger$  are the fermionic operators that diagonalize the Hamiltonian  $H(\lambda_i^{(2)})$  and we define

$$\chi_k = \theta_k(\lambda_i^{(1)}) - \theta_k(\lambda_i^{(2)}). \quad (20)$$

After a straightforward calculation, we obtain

$$\mathcal{F}(\lambda_x, \lambda_y, h; \lambda'_x, \lambda'_y, h') = \prod_{0 \leq k \leq \pi} \left| \cos\left(\frac{\theta_k - \theta'_k}{2}\right) \right|.$$

From this expression, we compute the quantum geometric tensor [31]

$$T_{ab} = \sum_{0 \leq k \leq \pi} \frac{1}{4} \frac{\partial \theta_k}{\partial \lambda_a} \frac{\partial \theta_k}{\partial \lambda_b}$$

using the convention  $\lambda_1 = \lambda_x$ ,  $\lambda_2 = \lambda_y$ , and  $\lambda_3 = h$ , where

$$\begin{aligned} \frac{\partial \theta_k}{\partial \lambda_x} &= -\frac{\cos(k)\delta_k - \sin(k)\epsilon_k}{\Delta_k^2}, \\ \frac{\partial \theta_k}{\partial \lambda_y} &= -\frac{\cos(k)\delta_k + \sin(k)\epsilon_k}{\Delta_k^2}, \quad \frac{\partial \theta_k}{\partial h} = -\frac{\delta_k}{\Delta_k^2}. \end{aligned}$$

Note that  $T_{ab}$  may not be analytic when the system becomes gapless, i.e., when  $\Delta_k \rightarrow 0$  for some  $k$ . Since  $T_{ab}$  is a real tensor, this system will have a trivial Berry curvature. The above expressions for the quantum geometric tensor are nontrivial. We expect to find a richness of features in their scaling behavior [31], which can potentially be of use in the optimization of quantum adiabatic algorithms [33]. A thorough study of the scaling of the geometric tensor in the cluster-XY model is to be found in Ref. [34].

By computing the fidelity in the cluster-XY model, we find the expected critical lines. We illustrate this in Fig. 2, plotting the phase diagram region that we already discussed in the context of the exact solution.

We notice that there is a set of multicritical points that present anomalous behavior. It is known that some multicritical points may behave differently, giving rise to anomalous dynamical scaling properties and, as a consequence, different universality classes [35,36]. The multicritical points  $\tilde{\lambda}^{(c)}$ , given by

$$(\lambda_x, \lambda_y, h) = \left( \pm \frac{h-3}{2}, \pm \frac{h+1}{2}, h \right) \quad \forall h \in \mathbb{R}, \quad (21)$$

have properties that are not present in other multicritical points, like the point  $(\lambda_x, \lambda_y, h) = (0, 1, 0)$  that was studied extensively in Ref. [25]. In fact, the overlap between the ground state corresponding to the critical points  $|\Omega(\lambda_i^{(c)})\rangle$  and the neighboring ground states is very large. Moreover, also the overlap  $F_1(\lambda'_i)$  between such multicritical ground states and the subspace generated by excited pairs  $\{\gamma_k^\dagger \gamma_{-k}^\dagger | \Omega(\lambda_i^{(c)})\rangle\}_k$  is quite large:

$$F_1(\lambda'_i) = \sum_{0 \leq k \leq \pi} \left| \langle \Omega(\lambda'_i) | \gamma_k^\dagger \gamma_{-k}^\dagger | \Omega(\lambda_i^{(c)}) \rangle \right|^2. \quad (22)$$

This overlap region will roughly follow the truncated surface given by Eq. (10).

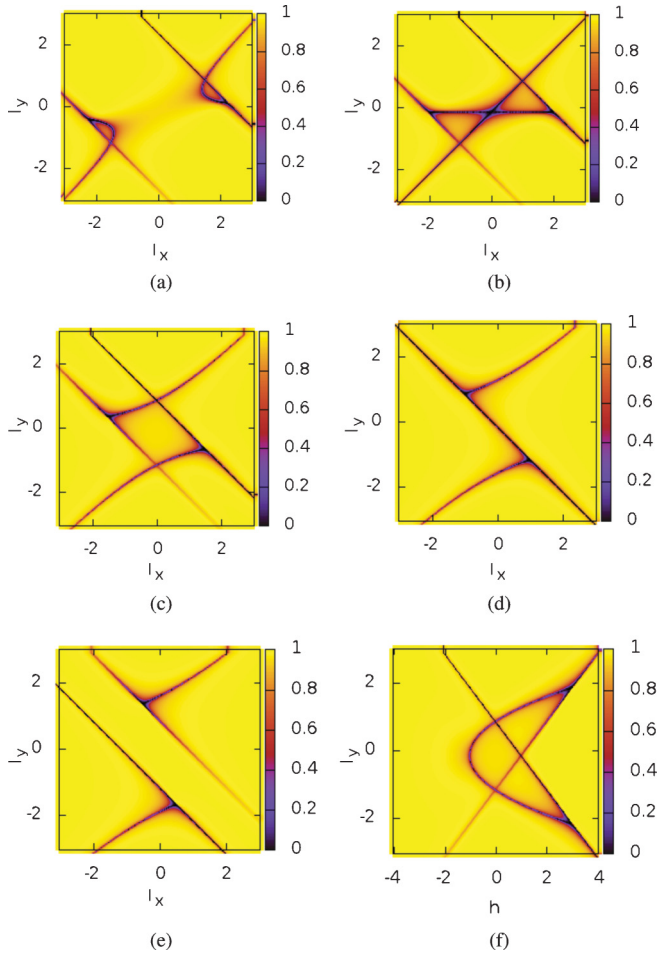


FIG. 2. (Color online) Contour plot of the fidelity  $\mathcal{F}(\lambda_y, \lambda_y + \delta\lambda_y)$ ,  $\delta\lambda_y = 0.05$ , and  $N = 500$  for constant  $h$ : (a)  $h = -1.5$ , (b)  $h = -1$ , (c)  $h = 0$ , (d)  $h = 1$ , and (e)  $h = 2$ . (f) Constant  $\lambda_x = 0$ .

We can gain some physical intuition about these multicritical if we rewrite the Hamiltonian as

$$\begin{aligned}
 H(h) = & 3 \left( \pm \sum_i \sigma_i^x \sigma_{i+1}^x + \sum_i \sigma_i^z \right) \\
 & + \left( - \sum_i \sigma_{i-1}^x \sigma_i^z \sigma_{i+1}^x \pm \sum_i \sigma_i^y \sigma_{i+1}^y \right) \\
 & + (h + 3) \left( \pm \frac{1}{2} \sum_i (\sigma_i^x \sigma_{i+1}^x + \sigma_i^y \sigma_{i+1}^y) - \sum_i \sigma_i^z \right).
 \end{aligned}$$

This corresponds to the sum of three critical Hamiltonians, namely, a critical Ising model, a critical cluster-Ising model, and a critical XX model with a transverse field. Note that for  $|h| \gg 1$ , the XX model term dominates. The ground state of this Hamiltonian corresponds, after a Jordan-Wigner transformation, to a completely empty (full) Fermi sea [1]. This state is trivial from the entanglement point of view since it corresponds to a product state [37], but it affects the behavior of the fidelity susceptibility in its vicinity [38,39].

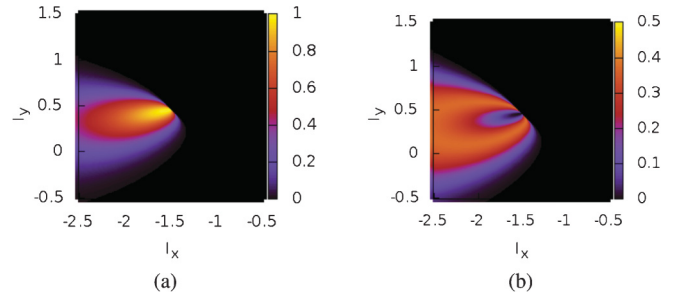


FIG. 3. (Color online) (a) Overlap between  $|\Omega(P1)\rangle$  and the neighboring ground states ( $N = 500$ ,  $q = 1$ , and  $h = 0$ ). (b) Overlap  $F_1(\lambda)$  between the two-particle states of  $P1$  and the neighboring ground states ( $N = 500$ ,  $q = 1$ , and  $h = 0$ ).

For the sake of concreteness we will concentrate on two of these points

$$(\lambda_x, \lambda_y, h) = \left(-\frac{3}{2}, \frac{1}{2}, 0\right) \quad (P1), \quad (23)$$

$$(\lambda_x, \lambda_y, h) = (-2, 0, -1) \quad (P2). \quad (24)$$

The overlap with the neighboring ground states is illustrated in Figs. 3 and 4. We see a significant overlap between the state at the quantum critical point and the neighboring ground states of the antiferromagnetic phase. This phenomenon is due to the fact that the perturbation corresponding to the parameter  $\lambda_i$  is not sufficiently relevant [31]. The overlap  $F_1(\lambda'_i)$  (22) is also considered, showing that the most significant overlap is with either the ground state or just a few pairs of excitations. Note that  $F_1$  is symmetric, so we also get the overlap between the subspace of a pair of excitations of the neighboring states and the critical point ground state.

The other critical points that do not belong to these critical lines present a behavior similar to the one obtained for the XY model in previous studies [27]. In those cases, the overlap with all the neighboring ground states decays very fast even for finite systems. In the present model, we expect this behavior for asymptotically large values of all the couplings  $\lambda_x$ ,  $\lambda_y$ , and  $h$  since the cluster interaction in the Hamiltonian (2) becomes negligible in comparison and we obtain the usual XY model. This fact implies that the two planes given by Eq. (9) correspond asymptotically to the Ising critical lines and the hyperbolic surface (10) corresponds asymptotically to the XX critical line. Note, however, that the universality class may be

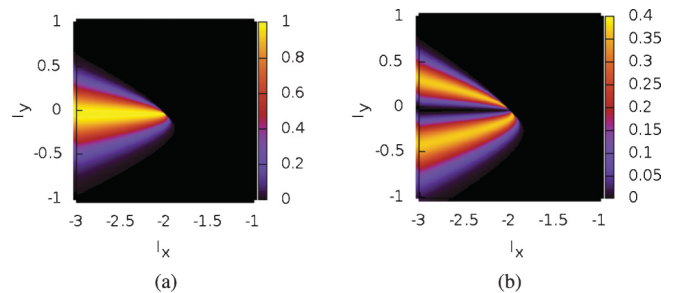


FIG. 4. (Color online) (a) Overlap between  $|\Omega(P2)\rangle$  and the neighboring ground states ( $N = 500$ ,  $q = 1$ , and  $h = -1$ ). (b) Overlap  $F_1(\lambda)$  between the two-particle states of  $P2$  and the neighboring ground states ( $N = 500$ ,  $q = 1$ , and  $h = -1$ ).

affected as we get close to the multicritical region we have been considering [36].

### V. QUANTUM QUENCHES AND LOSCHMIDT ECHO

At this point, we are ready to study the dynamics of the system after a quantum quench. In order to quantify this we use the Loschmidt echo (LE). This quantity is widely used in many-body physics, in particular in the field of quantum

chaos [11–14]. Suppose we want to compare the dynamics under the Hamiltonians  $H_1$  and  $H_2$  (possibly time dependent) imposing the same initial conditions  $|\psi(t=0)\rangle = |\psi_0\rangle$ . In that case, we define the LE as

$$\mathcal{L}(\psi_0, t) = |\langle \psi_0 | U_1(-t) U_2(t) | \psi_0 \rangle|^2, \quad (25)$$

where  $U_a(t) = \hat{T} \exp[-i \int_0^t H_a(t') dt']$  and  $\hat{T}$  denotes time ordering. Note that  $\mathcal{L}(t=0) = 1$ . In this paper, we will limit ourselves to ground states of one of the Hamiltonians, so that one of the unitaries in Eq. (25) acts trivially. This can be interpreted operationally as preparing the system in the ground state of the Hamiltonian with parameters  $\lambda_i^{(1)}$ , suddenly switching  $\lambda_i^{(1)} \rightarrow \lambda_i^{(2)}$ , and letting the system evolve with the new Hamiltonian. The LE reads

$$\mathcal{L}(\lambda_i^{(1)}, \lambda_i^{(2)}, t) = |\langle \Omega(\lambda_i^{(1)}) | U(t) | \Omega(\lambda_i^{(1)}) \rangle|^2. \quad (26)$$

In this sense, the LE is a dynamical version of the ground-state fidelity. High values of the LE mean that the system is approaching the initial state. Typically, the LE will decay exponentially at first and then start oscillating around a well-defined value [13,14]. If the system is finite, we expect the time evolution to be quasiperiodic, driving the system arbitrarily close to the initial state for long enough times. The system will experience revivals, i.e., times when the value of the LE is greater than two standard deviations from the average. The structure of these revivals may be greatly affected by criticality [15]. The time evolution in the cluster-XY model after a quantum quench is given by

$$|\psi(t)\rangle = \prod_{0 \leq k \leq \pi} \left[ \cos\left(\frac{\chi_k}{2}\right) + i e^{-i4t\Delta_k} \sin\left(\frac{\chi_k}{2}\right) \gamma_k^\dagger \gamma_{-k}^\dagger \right] |\Omega(\lambda_i^{(2)})\rangle \quad (27)$$

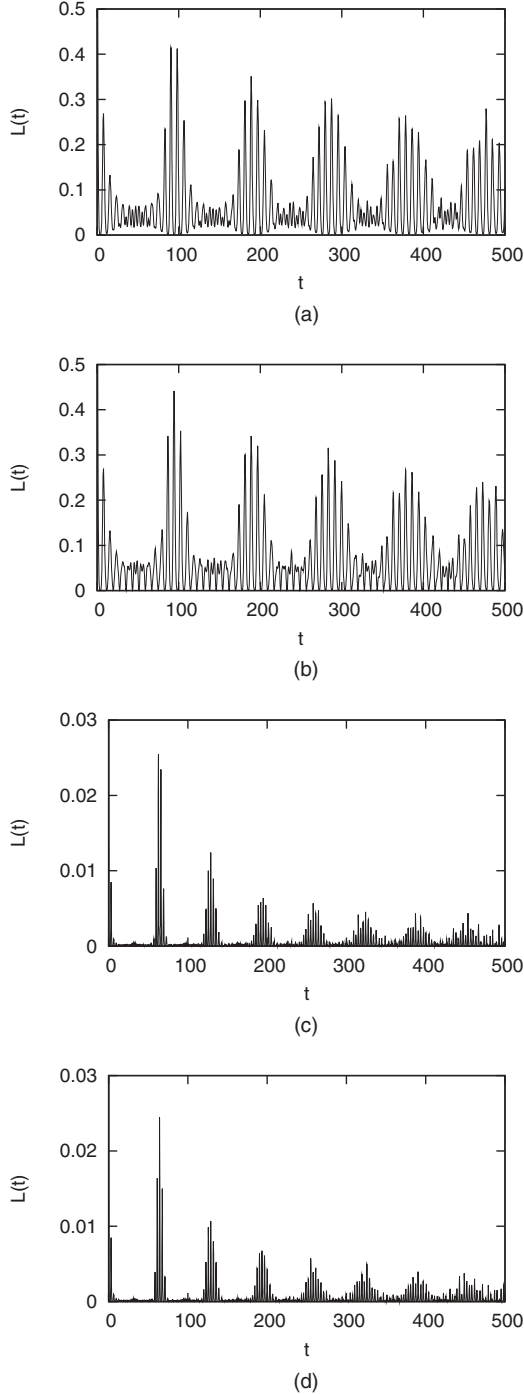


FIG. 5. The LE starting from the cluster phase to the critical point  $\lambda_x = -\frac{3}{2}$ ,  $\lambda_y = \frac{1}{2}$ , and  $h = 0$  with  $N = 400$  starting from  $(\lambda_y$  and  $h$  kept fixed) (a)  $\lambda_x = -1.3$ ,  $q = 1$ , (b)  $\lambda_x = -1.3$ ,  $q = 0$ , (c)  $\lambda_x = -1$ ,  $q = 1$ , and (d)  $\lambda_x = -1$ ,  $q = 0$ .

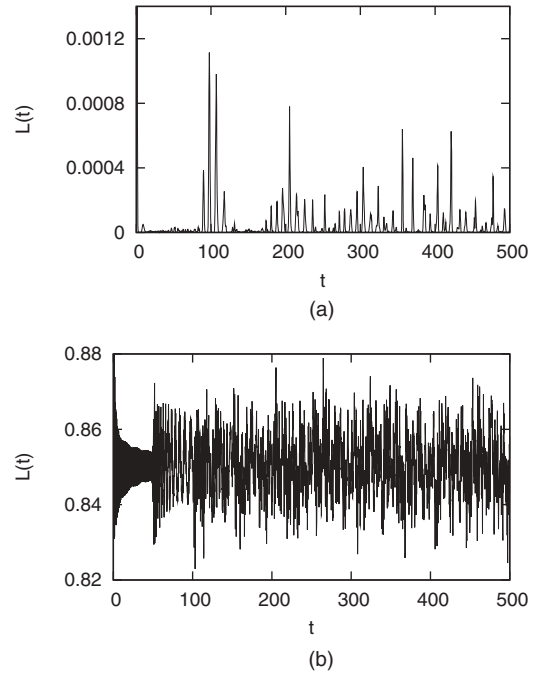


FIG. 6. The LE for the quenched cluster-Ising model to the critical point  $\lambda_x = -\frac{3}{2}$ ,  $\lambda_y = \frac{1}{2}$ , and  $h = 0$  with  $N = 400$  starting from (a)  $\lambda_y = 0.7$ ,  $q = 1$  ( $\lambda_x$  and  $h$  kept fixed, polarized) and (b)  $\lambda_x = -1.7$ ,  $q = 1$  ( $\lambda_y$  and  $h$  kept fixed, ferromagnetic).

and the LE is thus

$$\begin{aligned} \mathcal{L}(t) &= |\langle \psi(t) | \psi(0) \rangle|^2 \\ &= \prod_{0 \leq k \leq \pi} [1 - \sin^2(\chi_k) \sin^2(2t \Delta_k)]. \end{aligned} \quad (28)$$

In the following, we show the detailed analysis of the LE for different types of quenches.

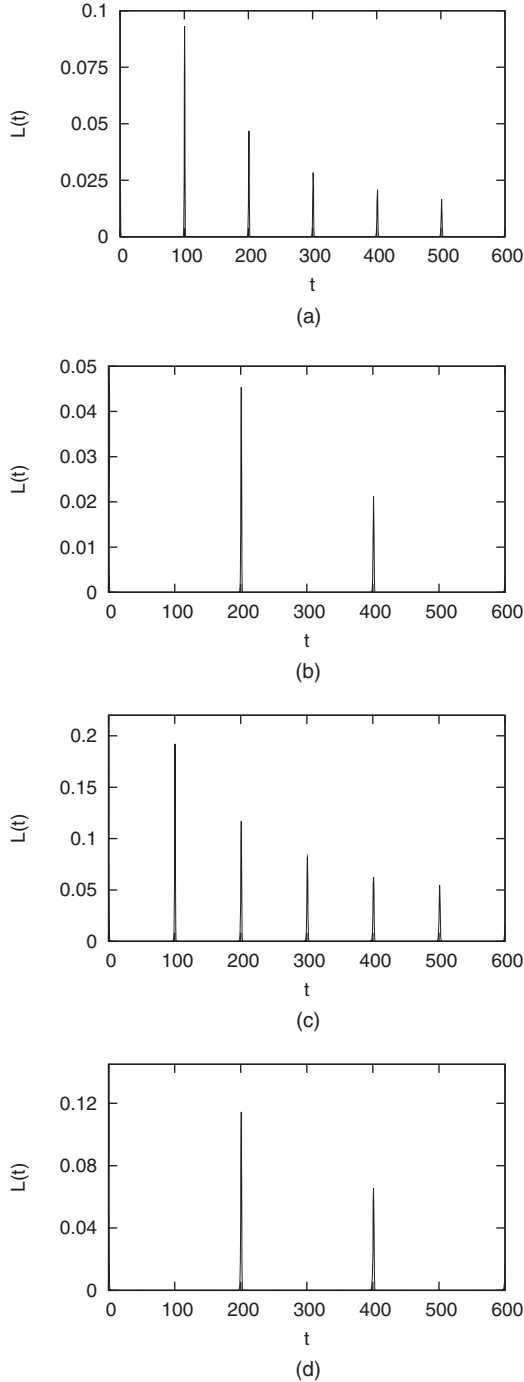


FIG. 7. The LE for the quenched cluster-Ising model to the critical point  $\lambda_x = 0$ ,  $\lambda_y = 1$ , and  $h = 0$  with  $N = 400$  starting from  $(\lambda_x$  and  $h$  kept fixed) (a)  $\lambda_y = 0.8$ ,  $q = 1$  (cluster), (b)  $\lambda_y = 0.8$ ,  $q = 0$  (cluster), (c)  $\lambda_y = 1.2$ ,  $q = 1$  (antiferromagnetic), and (d)  $\lambda_y = 1.2$ ,  $q = 0$  (antiferromagnetic).

Consider the critical point  $h = 0$ ,  $\lambda_x = -\frac{3}{2}$ ,  $\lambda_y = \frac{1}{2}$ . The critical Hamiltonian is

$$H = - \sum_{i=1}^N \sigma_{i-1}^x \sigma_i^z \sigma_{i+1}^x - \frac{3}{2} \sum_{i=1}^N \sigma_i^x \sigma_{i+1}^x + \frac{1}{2} \sum_{i=1}^N \sigma_i^y \sigma_{i+1}^y.$$

As we see in Fig. 1(b), this point lies between three different phases. If we increase  $\lambda_x$  ( $\lambda_y$ ) we will be in the cluster (polarized) phase. Decreasing  $\lambda_y$  or  $\lambda_x$  results in a ferromagnetic state in the  $x$  direction.

For this critical point the behavior of the LE depends on which phase the system is prepared in. For the cluster state (Fig. 5) the numerical simulations show that it will oscillate strongly away from the mean value. We also get a noticeable spreading of the revivals. If we start further from the critical point (i.e., a stronger quench), the lines get closer, but we keep the insensitivity to the parity of the ground state [ $Q = (-1)^q$ ]. Note that the stronger the quench, the sooner the revivals will happen. If we start from the polarized phase [Fig. 6(a)], the behavior of the LE is somewhat different. Once again, the oscillations make the revival structure insensitive to the parity sector.

In contrast, starting from the ferromagnetic phase changes the LE completely [Fig. 6(b)]. The numerical simulations show that it will oscillate randomly around a relatively high mean value. There is no outstanding structure for the revivals as we had in the previous quenches. Increasing the size of the quench will give us basically the same result, only decreasing the mean value. This is consistent with the significant overlap of the ground state of this critical point with the neighboring ferromagnetic ground states [Fig. 3(a)].

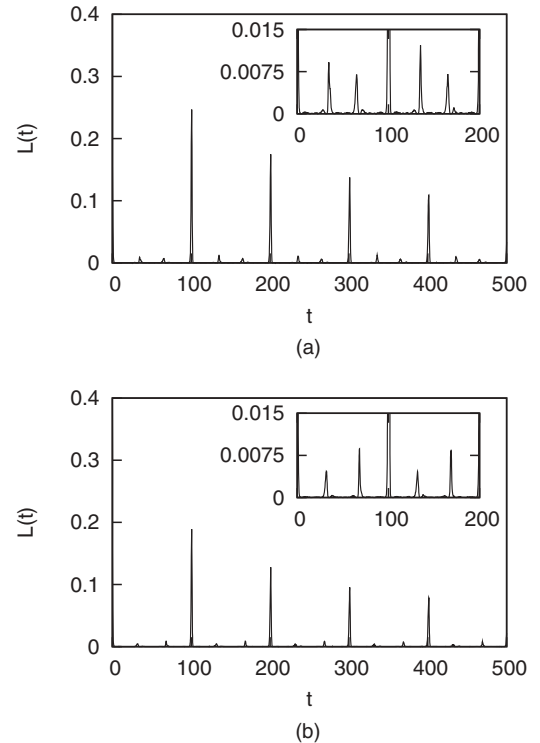


FIG. 8. The LE for the quenched cluster-Ising model to the critical point  $\lambda_x = 0$ ,  $\lambda_y = 1$ , and  $h = 0$  with  $N = 400$  starting from  $(\lambda_y$  and  $h$  kept fixed) (a)  $\lambda_x = -0.2$ ,  $q = 1$  and (b)  $\lambda_x = 0.2$ ,  $q = 1$ .

Consider now  $h = 0$ ,  $\lambda_x = 0$ ,  $\lambda_y = 1$ . For these values, the critical Hamiltonian is

$$H = - \sum_{i=1}^N \sigma_{i-1}^x \sigma_i^z \sigma_{i+1}^x + \sum_{i=1}^N \sigma_i^y \sigma_{i+1}^y.$$

This critical point lies on the interface of four different phases [Fig. 1(b)]. If  $\lambda_y$  is increased, we will be in a region that can be connected to an antiferromagnet in the  $y$  direction. If  $\lambda_y$  is decreased, we will be in the cluster region. A positive  $\lambda_x$  will turn the system into an antiferromagnet in the  $x$  direction, while a small negative  $\lambda_x$  will put it in a region that can be connected to a separable state polarized in the  $z$  direction.

The behavior of the LE after a quench of  $\lambda_y$  (Fig. 7) is similar to the one obtained for critical quenches in the  $XY$  model [16]. It features the same sensitivity to the parity that cancels the odd revivals for even parity ( $q = 0$ ). This can

be understood easily by noting that for  $k = \pi/N$  and  $t = \frac{N}{4} |\frac{\partial \Delta_k}{\partial k}|_{\max}^{-1}$ , we get  $\chi_k \sim \frac{\pi}{2}$  (as can be seen in the fidelity) and  $2t \Delta_k \sim \frac{\pi}{2}$ , canceling the LE [Eq. (28)].

Starting with a small nonzero value for  $\lambda_x$  and quenching the system to this critical point, the LE will behave roughly in the same way (Fig. 8). However, we get two small peaks before the first revival. Strictly speaking, they will not be revivals according to the definition because they are less than two standard deviations away from the mean value of the LE. We can understand them as dynamical responses given by the Bogoliubov quasiparticles.

We can also quench to the neighboring critical points along the critical curve  $\lambda_y^2 - \lambda_x \lambda_y - 1 = 0$  (see Fig. 9). This means that both the starting and quenching Hamiltonians lie on this curve. In this case, the main difference will be the revival time, which will be exactly one-third of the one found in the previous quenches. Note that we do not get this phenomenon for the critical line  $\lambda_y = -\lambda_x + 1$ ,  $h = 0$ .

In Ref. [16], the phenomenon of the revivals after a quantum quench is interpreted as a recombination of the fastest quasiparticles in the system. In general, the fastest excitations in the system have a speed that is upper bounded by the Lieb-Robinson speed  $v_{LR}$  [40–42]. This upper bound gives a lower bound to the revival time  $T_{rev} \gtrsim \frac{N}{2v_{LR}}$ . Following Ref. [43], we find  $v_{LR} \simeq 3.2e/\sqrt{2} = 6.15$  for the critical point  $\lambda_y = 1$ ,  $\lambda_x = 0$ , and  $h = 0$  and therefore the maximum speed of quasiparticles given by the maximum group velocity  $2\partial_k \Delta_k|_{\max} = 6$  [Fig. 9(d)] is compatible with the Lieb-Robinson bound.

## VI. CONCLUSION

In this paper, we studied the phase diagram and quench behavior of the cluster- $XY$  model, a spin chain where the usual  $XY$  interactions in a transverse field are competing with a cluster three-body term. This model also describes the effective behavior of the edge in a two-dimensional fermionic symmetry-protected topological state with  $Z_2$  symmetry [44]. The cluster- $XY$  model is exactly solvable by standard techniques and the study has been conducted using the tools of fidelity susceptibility and Loschmidt echo. This model, inspired by proposed implementations of quantum computation, provides a benchmark with an interesting phenomenology and a much richer phase space resulting from the competition of the different interactions. We were able to characterize the critical regions and the distribution of phases using the quantum geometric tensor. We found that the phase diagram is completely characterized by the fidelity. It is noteworthy that the ground state of some of the critical points presents a large overlap with the ground state and few-excitation subspaces of neighboring noncritical regions. The behavior away from equilibrium is also nontrivial. We showed that different critical points have qualitatively different effects on the LE. The long-time structure and the revival times of the LE depend on the initial phase of the quantum quench and the final critical point. This provides further phenomenology for the study of generic responses to critical quantum quenches.

In Refs. [24,45] it was shown that the cluster-Ising model with open boundary conditions has a fourfold degenerate

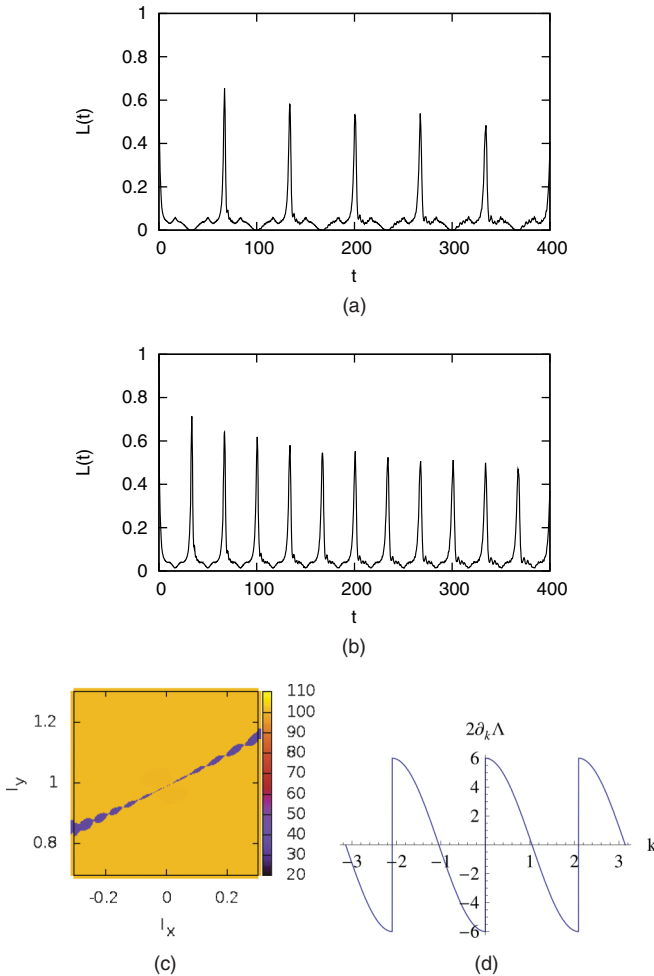


FIG. 9. (Color online) The LE for the quench to the critical point  $\lambda_x = 0$ ,  $\lambda_y = 1$ , and  $h = 0$  along the critical line  $\lambda_y^2 - \lambda_x \lambda_y - 1 = 0$  with  $N = 400$  starting from  $(\lambda_x, \lambda_y)$  along the critical line and  $h = 0$  kept fixed) (a)  $\lambda_x = 0.1$ ,  $q = 0$  (notice that the revivals with odd parity are destroyed by interference) and (b)  $\lambda_x = 0.1$ ,  $q = 1$ . (c) Revival time for critical quenches to the same critical point starting in the neighboring ground states. Notice that the critical line is detected by the revival time. (d) Group velocity  $2\partial_k \Delta_k$  for the critical point. The maximum value is  $2\partial_k \Delta_k|_{\max} = 6$ .

ground space that possesses symmetry-protected topological order [46–48]. We expect that this model has similar features [34], though the presence of the nontrivial phases between the cluster phase and the ferromagnetic phase makes the situation more complicated. A promising route to the characterization of topological orders is the study of their entanglement spectrum [49,50]. In a symmetry-protected one-dimensional spin-one chain in the Haldane phase, the topological order is revealed in a double degeneracy of the entanglement spectrum [51]. It would hence be interesting to study the entanglement spectrum of the cluster-XY model to gain more insight into the properties of the symmetry-protected topological order. In particular, it would be interesting to study the robustness of the information encoded in such ground space after a quantum quench and

whether or not the quench breaks the symmetry that protects the topological order. Finally, it would be interesting to study the model in the presence of disorder. In order to obtain reliable results, more sophisticated numerical techniques may be used such as matrix product states.

#### ACKNOWLEDGMENTS

S.M. would like to thank Felix Flicker, Holger Haas, Guifré Vidal, and Marek Rams for useful discussions. Research at Perimeter Institute for Theoretical Physics was supported in part by the Government of Canada through Natural Sciences and Engineering Research Council and by the Province of Ontario through Ministry of Research and Innovation.

- 
- [1] S. Sachdev, *Quantum Phase Transitions* (Cambridge University Press, Cambridge, 1999).
- [2] L. Amico, R. Fazio, A. Osterloh, and V. Vedral, *Rev. Mod. Phys.* **80**, 517 (2008).
- [3] X.-G. Wen, *Quantum Field Theory of Many-Body Systems* (Oxford University Press, Oxford, 2004).
- [4] M. Greiner, O. Mandel, T. Esslinger, T. W. Hänsch, and I. Bloch, *Nature (London)* **415**, 39 (2002).
- [5] M. Greiner, O. Mandel, T. W. Hänsch, and I. Bloch, *Nature (London)* **419**, 51 (2002).
- [6] I. Bloch, J. Dalibard, and W. Zwerger, *Rev. Mod. Phys.* **80**, 885 (2008).
- [7] S. Popescu, A. J. Short, and A. Winter, *Nat. Phys.* **2**, 754 (2006).
- [8] N. Linden, S. Popescu, A. J. Short, and A. Winter, *Phys. Rev. E* **79**, 061103 (2009).
- [9] A. Polkovnikov, K. Sengupta, A. Silva, and M. Vengalattore, *Rev. Mod. Phys.* **83**, 863 (2011).
- [10] *Quantum Quenching, Annealing and Computation*, edited by A. K. Chandra, A. Das, and B. K. Chakrabarti (Springer, Heidelberg, 2010).
- [11] T. Gorin, T. Prosen, T. H. Seligman, and M. Znidaric, *Phys. Rep.* **435**, 33 (2006).
- [12] Ph. Jacquod and C. Petitjean, *Adv. Phys.* **58**, 67 (2009).
- [13] L. Campos Venuti and P. Zanardi, *Phys. Rev. A* **81**, 022113 (2010).
- [14] L. Campos Venuti, N. T. Jacobson, S. Santra, and P. Zanardi, *Phys. Rev. Lett.* **107**, 010403 (2011).
- [15] H. T. Quan, Z. Song, X. F. Liu, P. Zanardi, and C. P. Sun, *Phys. Rev. Lett.* **96**, 140604 (2006).
- [16] J. Häppölä, G. B. Halász, and A. Hamma, *Phys. Rev. A* **85**, 032114 (2012).
- [17] R. Raussendorf, D. E. Browne, and H. J. Briegel, *Phys. Rev. A* **68**, 022312 (2003).
- [18] S. D. Bartlett and T. Rudolph, *Phys. Rev. A* **74**, 040302(R) (2006).
- [19] H. J. Briegel, D. E. Browne, W. Dür, R. Raussendorf, and M. Van den Nest, *Nat. Phys.* **5**, 19 (2009).
- [20] T.-C. Wei, I. Affleck, and R. Raussendorf, *Phys. Rev. Lett.* **106**, 070501 (2011).
- [21] A. Miyake, *Ann. Phys. (Leipzig)* **326**, 1656 (2011).
- [22] S. O. Skrøvseth and S. D. Bartlett, *Phys. Rev. A* **80**, 022316 (2009).
- [23] A. C. Doherty and S. D. Bartlett, *Phys. Rev. Lett.* **103**, 020506 (2009).
- [24] W. Son, L. Amico, R. Fazio, A. Hamma, S. Pascazio, and V. Vedral, *Europhys. Lett.* **95**, 50001 (2011).
- [25] P. Smacchia, L. Amico, P. Facchi, R. Fazio, G. Florio, S. Pascazio, and V. Vedral, *Phys. Rev. A* **84**, 022304 (2011).
- [26] P. Zanardi, P. Giorda, and M. Cozzini, *Phys. Rev. Lett.* **99**, 100603 (2007).
- [27] P. Zanardi and N. Paunković, *Phys. Rev. E* **74**, 031123 (2006).
- [28] P. W. Anderson, *Phys. Rev. Lett.* **18**, 1049 (1967).
- [29] S.-J. Gu, *Int. J. Mod. Phys. B* **24**, 4371 (2010).
- [30] A. Polkovnikov and V. Gritsev, in *Understanding Quantum Phase Transitions*, edited by L. D. Carr (Taylor & Francis, Boca Raton, FL, 2011).
- [31] L. Campos Venuti and P. Zanardi, *Phys. Rev. Lett.* **99**, 095701 (2007).
- [32] A. Hamma, [arXiv:quant-ph/0602091v1](https://arxiv.org/abs/quant-ph/0602091v1).
- [33] A. T. Rezakhani, W.-J. Kuo, A. Hamma, D. A. Lidar, and P. Zanardi, *Phys. Rev. Lett.* **103**, 080502 (2009).
- [34] A. Hamma *et al.*, in preparation.
- [35] V. Mukherjee, U. Divakaran, A. Dutta, and D. Sen, *Phys. Rev. B* **76**, 174303 (2007).
- [36] S. Deng, G. Ortiz, and L. Viola, *Phys. Rev. B* **80**, 241109(R) (2009).
- [37] J. I. Latorre, E. Rico, and G. Vidal, *Quantum Inf. Comput.* **4**, 48 (2004).
- [38] V. Mukherjee, A. Polkovnikov, and A. Dutta, *Phys. Rev. B* **83**, 075118 (2011).
- [39] M. M. Rams and B. Damski, *Phys. Rev. A* **84**, 032324 (2011).
- [40] E. H. Lieb and D. W. Robinson, *Commun. Math. Phys.* **28**, 251 (1972).
- [41] B. Nachtergaele, Y. Ogata, and R. Sims, *J. Stat. Phys.* **124**, 1 (2006).
- [42] I. Prémont-Schwarz and J. Hnybida, *Phys. Rev. A* **81**, 062107 (2010).
- [43] A. Hamma, F. Markopoulou, I. Prémont-Schwarz, and S. Severini, *Phys. Rev. Lett.* **102**, 017204 (2009).
- [44] Z.-C. Gu and X.-G. Wen, [arXiv:1201.2648v1](https://arxiv.org/abs/1201.2648v1).
- [45] W. Son, L. Amico, and V. Vedral, *Quantum Inf. Process.* **1** (2011).

- [46] S. P. Kou and X.-G. Wen, *Phys. Rev. B* **80**, 224406 (2009).
- [47] Z.-X. Liu, X. Chen, and X.-G. Wen, *Phys. Rev. B* **84**, 195145 (2011).
- [48] F. Pollmann, E. Berg, A. M. Turner, and M. Oshikawa, *Phys. Rev. B* **85**, 075125 (2012).
- [49] H. Li and F. D. M. Haldane, *Phys. Rev. Lett.* **101**, 010504 (2008).
- [50] S. T. Flammia, A. Hamma, T. L. Hughes, and X.-G. Wen, *Phys. Rev. Lett.* **103**, 261601 (2009).
- [51] F. Pollmann, A. M. Turner, E. Berg, and M. Oshikawa, *Phys. Rev. B* **81**, 064439 (2010).